

Original Article

Oncostatin M promotes infarct repair and improves cardiac function after myocardial infarction

Hui Han^{1,2*}, Daopeng Dai^{1,2*}, Run Du^{1*}, Jinquan Hu³, Zhengbin Zhu¹, Lin Lu^{1,2}, Jinzhou Zhu¹, Ruiyan Zhang^{1,2}

¹Department of Cardiovascular Medicine, Ruijin Hospital, Shanghai Jiao Tong University School of Medicine, Shanghai 200025, P. R. China; ²Institute of Cardiovascular Diseases, Shanghai Jiao Tong University School of Medicine, Shanghai 200025, P. R. China; ³Department of Orthopaedics, Changzheng Hospital Affiliated with Second Military Medical University, Shanghai 200003, P. R. China. *Equal contributors.

Received December 28, 2020; Accepted August 7, 2021; Epub October 15, 2021; Published October 30, 2021

Abstract: Myocardial infarction (MI) is one of the leading causes of morbidity and mortality worldwide. The immune response plays a central role in post-MI cardiac repair. A growing body of evidence suggests that oncostatin M (OSM), a pleiomorphic cytokine of the interleukin (IL)-6 family, participates in the cardiac healing and remodeling process. However, previous studies have shown inconsistent results, and the exact mechanisms underlying this process have not yet been fully elucidated. We verified whether OSM is involved in the healing process and cardiac remodeling after MI and sought to explore its potential mechanisms. Our data implied OSM's role in facilitating the post-MI healing process in mice, manifested by improved cardiac functional performance and a reduction in fibrotic changes. Furthermore, our flow cytometry analysis revealed that OSM influences the dynamics of cardiac monocytes and macrophages. In mice with a blunted C-X-C motif receptor (CCR)2 signaling pathway, OSM reserved its protective roles and polarized cardiac macrophages toward a reparative phenotype. Moreover, OSM reduced the number of matrix metalloproteinase (MMP)-9⁺ immune cells and increased the number of tissue inhibitor of metalloproteinase (TIMP)-1⁺ immune cells in the infarct area, mitigating the maladaptive remodeling following MI. These findings demonstrate that OSM favorably modulates cardiac remodeling, partially by accelerating the shift in the cardiac macrophage phenotype from M1 to M2 and by correcting the MMP-9 and TIMP-1 balance.

Keywords: Myocardial infarction, oncostatin M, cardiac remodeling, immune response, macrophage polarization

Introduction

Myocardial infarction (MI), induced by temporary or permanent thrombosis in the coronary arteries, is one of the leading causes of morbidity and mortality worldwide [1]. Timely thrombolysis, balloon dilatation, and stent implantation into the culprit vessel have been shown to be effective at reducing the necrotic area and improving the survival rate of MI [2, 3]. However, many survivors go on to develop myocardial dysfunction or heart failure after MI [4, 5]. The immune response plays a central role in the healing process following acute MI (AMI). Monocytes and macrophages, pleiotropic cells of the innate immune system, play critical roles in the homeostatic maintenance of the myocardium under normal conditions and in response to injury. Following MI, the number of cardiac monocytes and macrophages expands rapidly

in the first few days. These initial populations demonstrate a pro-inflammatory phenotype, which shifts over the ensuing days to a predominantly reparative phenotype that is key in orchestrating the repair response. During this process, improper early and prolonged inflammatory responses can disturb the balance between matrix degradation and collagen deposition, which contributes to impaired healing, harmful cardiac remodeling, and negative outcomes. Strategies targeting these subpopulations of macrophages may be able to favorably modulate the cardiac remodeling process after MI.

Oncostatin M (OSM), produced by activated T lymphocytes, monocytes/macrophages, and dendritic cells, is a pleiomorphic cytokine that belongs to the glycoprotein (gp) 130/IL-6-family of cytokines [6, 7]. OSM may have a role in

Oncostatin M protects the myocardium against myocardial ischemia

immune and inflammatory responses; however, inconsistent results have been shown in the cardiac healing and remodeling processes after acute and chronic heart injuries, although a limited number of studies have suggested that OSM might facilitate cardiomyocyte de-differentiation, regulate cardiomyocyte-dependent macrophage trafficking, promote autophagy, and suppress fibrogenesis [8-11]. While the observed dichotomy appears to be partially attributed to differences in the induction of heart injuries, the exact mechanisms remain to be fully illustrated.

In this study, the protective roles of OSM were verified using a post-MI mice model, and the dynamics of cardiac monocytes/macrophages in post-MI hearts were tested to explore their potential mechanisms. We demonstrated that OSM facilitates the healing process and improves the performance of the damaged left ventricle after MI by partially regulating the polarization of the cardiac monocytes/macrophages, especially resident macrophages.

Materials and methods

Induction of MI and drug treatment

Male C57BL/6J mice aged 6 weeks were purchased from the Model Animal Research Center of Nanjing University (Nanjing, People's Republic of China). The experimental animals were kept in a specific pathogen-free facility under a 12-h light/dark cycle with free access to water and food. The mice underwent a permanent ligation of the left anterior descending artery (LAD) or sham operations after 1 week of acclimatization, as described previously [12, 13]. Briefly, the mice were anesthetized with 2.0% isoflurane gas, and a rodent respirator was used to assist the mechanical ventilation. The chest cavity was opened using a left thoracotomy so that the heart could be exposed and the LAD could be visualized using a microscope. The LAD was permanently ligated at the site of its emergence from the left atrium with a 7-0 silk suture. The presence of myocardial blanching in the perfusion bed confirmed the complete occlusion of the blood vessels. The sham-operated animals underwent the same procedure without coronary artery ligation. The mice that did not survive the surgery were excluded from further analysis. The mice were anesthetized using 5% isoflurane and sacrificed by cervical dislocation at each experimen-

tal time point, and the tissues were obtained after the cardiac arrest in each mouse was confirmed. The animal experimental protocol complied with the Animal Management Rules of the Chinese Ministry of Health (document No. 55, 2001) and was approved by the Animal Care Committee of Shanghai Jiao Tong University (Permit Number: [2019]-12). The mice were fed in the Experimental Animal Center of Shanghai Jiaotong University School of Medicine, where the animal experiments were performed.

Experimental protocol

Two animal studies were performed in the current study. In animal study 1, C57BL/6J mice were used to clarify the role of OSM in the post-MI cardiac inflammation response and remodeling. In animal study 2, a CCR2 antagonist was used to impede the infiltration of blood monocytes, and the role of OSM on the resident macrophages was explored.

For animal study 1, the experimental mice were randomly divided into four groups as follows: (1) the sham-operated and vehicle-treated mice (sham + vehicle), (2) the sham-operated and OSM-treated mice (sham + OSM), (3) the MI model and vehicle-treated mice (MI + vehicle), and (4) the MI model and OSM-treated mice (MI + OSM). Before conducting the surgical procedures, recombinant mouse OSM (60 µg/kg) was dissolved in dimethyl sulfoxide and injected intraperitoneally twice a day for 14 days into the OSM mice [10]. The sham and MI groups were administered the same volume of dimethyl sulfoxide for 14 days. The recombinant mouse OSM (catalog No. 495-MO-025) was purchased from R&D Systems (Minneapolis, MN, USA).

For animal study 2, the CCR2 antagonist (RS504393 [RS]) was purchased from Tocris Bioscience (Tocris Cookson, Ellisville, MO, USA) and was administered subcutaneously (2 mg/kg/d) for 3 days before the LAD ligation until the end of the experiments. The RS-treated MI mice were then divided into two groups based on whether they received the vehicle or the OSM treatment: the MI + RS + vehicle group and the MI + RS + OSM group.

Echocardiography analysis

Fourteen days after the surgeries, transthoracic echocardiographies were performed to eval-

Oncostatin M protects the myocardium against myocardial ischemia

uate the cardiac function using a high-resolution ultrasound imaging system (Vevo 2100; FUJIFILM VisualSonics, Inc.). The left ventricular (LV) end-systolic diameters and the end-diastolic diameters were measured using M-mode tracings. The LV end-systolic volumes and the end-diastolic volumes were calculated as described previously [14]. The ejection fraction (EF) and fractional shortening (FS) were calculated using the following formulas: $EF (\%) = [(LVEDV - LVESV)/LVEDV] \times 100\%$ and $FS (\%) = [(LVEDD - LVESD)/LVEDD] \times 100\%$, where LVESD is the LV end-systolic diameter, LVEDD is the LV end-diastolic diameter, LVESV is the LV end-systolic volume, and LVEDV is the LV end-diastolic volume. The M-mode measurement data represent 3-6 averaged cardiac cycles from at least two scans per mouse.

Histological analysis

Masson's trichrome-staining procedure was performed on 6- μ m sections of the paraffin-embedded hearts to evaluate the severity of the cardiac fibrosis. The sections were photographed using an Olympus BX61 microscope (Olympus, Tokyo, Japan), and the percentages of staining in the sections were quantitatively analyzed using Image Pro Plus 6.0 software (Media Cybernetics, Inc., Rockville, MD, USA). The severity of cardiac fibrosis was indicated by the ratio of positively stained area to the total selected field.

For the immunofluorescence, the sections were incubated with primary anti-MMP-9 (1:100) or anti-TIMP-1 (1:100) antibodies overnight at 4°C. Next, the sections were incubated with Alexa Fluor® 488-conjugated secondary antibody (1:1000) at room temperature for 1 h and counterstained with 4,6-diamidino-2-phenylindole (DAPI).

The primary antibodies anti-TIMP-1 and anti-MMP-9 (catalog Nos. ab38978 and ab38898, respectively) were purchased from Abcam (Cambridge, MA, USA). The Alexa Fluor® 488-conjugated secondary antibody (catalog No. A11008) was purchased from ThermoFisher (Waltham, MA, USA).

Flow cytometry

For the heart sample preparation, all the anaesthetized mice underwent a thorax opening.

Their hearts were obtained for the subsequent flow cytometry procedures after PBS perfusion, as previously described [15]. Briefly, the heart was exposed, and a perfusion tube was inserted into the left ventricle. The right atrium was cut open before the PBS perfusion. The heart tissue samples were collected when the effluent from the right atrium was transparent and clear; then the samples were minced and dissolved in RPMI 1640 medium containing 8.5 U/ml DNase I (Roche) and 40 mg/ml Liberase™ (Roche, Basel, Switzerland) for 40 min at 37°C. The dissociation was terminated with serum-free RPMI 1640 medium. The erythrocytes were then lysed using a lysis buffer (RBC Lysis Buffer; eBioscience, San Diego, CA, USA). Following the lysis, the cells were resuspended in a FACS buffer (phosphate buffer saline). Subsequently, the cells were labeled with a mixture of antibodies for 30 min in the dark at 4°C. All the antibodies were used at a dilution of 1:100. Multi-color flow cytometry was performed on a flow cytometer (FACS Aria III; BD Biosciences, San José, USA) and analyzed using FlowJo software (Tree Star, Ashland, OR, USA).

The detailed antibody combinations for the flow cytometry were as follows: anti-CD11b-PerCP-cy5.5, anti-Ly6-G-APC, anti-CD45-FITC, anti-CD3-APC, and anti-CD19-PE (for the analyses presented in **Figure 2**); anti-CD45-FITC, anti-Ly6-G-APC, anti-F4/80-PerCP-cy5.5, and anti-Ly6-C-PE (for the analyses presented in **Figure 3**); anti-CD11b-FITC, anti-Ly6-G-APC, and anti-CD206-Alexa Fluor® 647 (for the analyses presented in **Figure 4**); and anti-CD11b-FITC, anti-MMP-9, anti-TIMP-1, and donkey anti-goat IgG (H+L)-PE (for the analyses presented in **Figure 5**).

Anti-CD11b-PerCP-Cy5.5 (catalog No. 561114), anti-CD11b-FITC (catalog No. 557396), anti-Ly6-G-APC (catalog No. 560599), anti-CD45-FITC (catalog No. 553079), anti-CD3-APC (catalog No. 553066), anti-CD19-PE (catalog No. 557399), anti-F4/80-PE (catalog No. 565410), anti-Ly6-C-PerCP-Cy5.5 (catalog No. 560525), and anti-CD206-Alexa Fluor® 647 (catalog No. 565250) were all purchased from BD Biosciences. Goat anti-MMP-9 (catalog No. AF909), goat anti-TIMP-1 (catalog No. AF980), and donkey anti-goat IgG (H+L) PE-conjugated antibody (catalog No. F0107) were all purchased from R&D Systems.

Oncostatin M protects the myocardium against myocardial ischemia

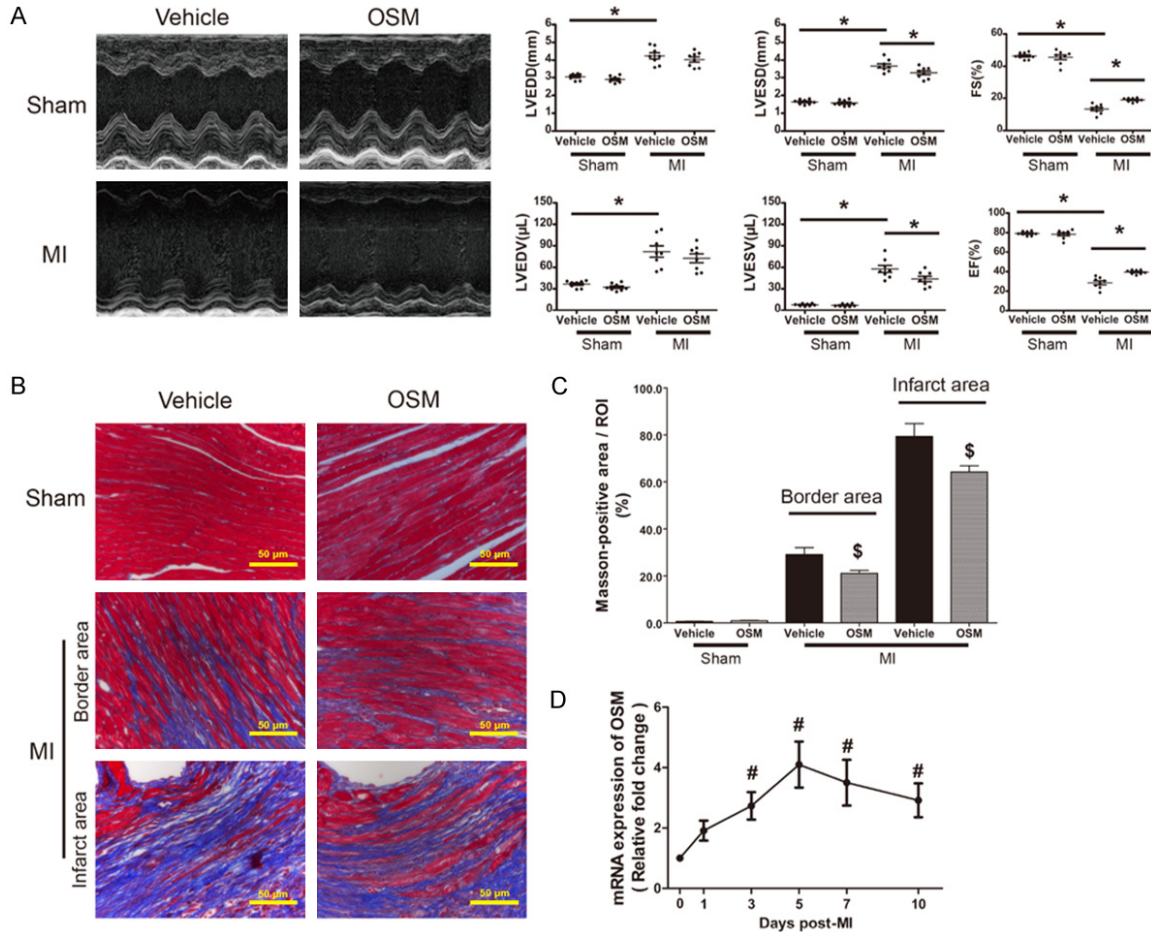


Figure 1. Oncostatin M (OSM) treatment contributes to the recovery of cardiac function from myocardial infarction (MI). **A.** Representative images of M-mode echocardiograms, and statistical analyses of LVEDD, LVESD, LVEDV, LVESV, FS, and EF in the sham + vehicle, sham + OSM, MI + vehicle, and MI + OSM mice. * $P < 0.05$ ($n = 8$). **B** and **C.** Representative images, and quantitative analyses of Masson's trichrome-stained sections in the hearts of the sham + vehicle, sham + OSM, MI + vehicle, and MI + OSM mice. * $P < 0.05$ ($n = 6$). The sections were photographed at 200 \times magnification. Scale bar = 50 μm . **D.** Time course of the mRNA expression of OSM after MI surgery for the wild-type mice. # $P < 0.05$ versus day 0 ($n = 6$). The data are presented as the mean \pm SEM.

Quantitative real-time polymerase chain reaction (PCR)

A Qiagen RNeasy kit was used to extract the total RNA according to the manufacturer's protocol. Reverse transcription of a total of 1 μg of RNA was performed using a reverse transcription system (Promega, Madison, WI, USA). Power SYBR Green PCR Master Mix in a StepOne (Applied BioSystems, Foster City, CA, USA) was used for the PCR amplification.

The following primers were used for real-time PCR: OSM (forward primer, 5'-TACCTGAGCCCA-CACAGACA-3'; reverse primer, 5'-CGATGGTATC-CCCAGAGAAA-3'), and β -actin (forward primer, 5'-CTGTCCTGTATGCCTCTG-3'; reverse primer,

5'-ATGTCACGCACGATTTC-3'). Gene expression levels were normalized with β -actin, and the data were analyzed using StepOne software v2.1 (Applied BioSystems, Foster City, CA, USA).

Statistical analysis

The continuous data were analyzed using unpaired or paired Student's t-tests and were presented as the means \pm standard error of the mean (SEM) unless otherwise stated. One-way analyses of variance followed by Bonferroni post-hoc analyses were performed to determine the differences among multiple groups. P -values < 0.05 were considered to indicate a statistically significant difference. SPSS 15.0

Oncostatin M protects the myocardium against myocardial ischemia

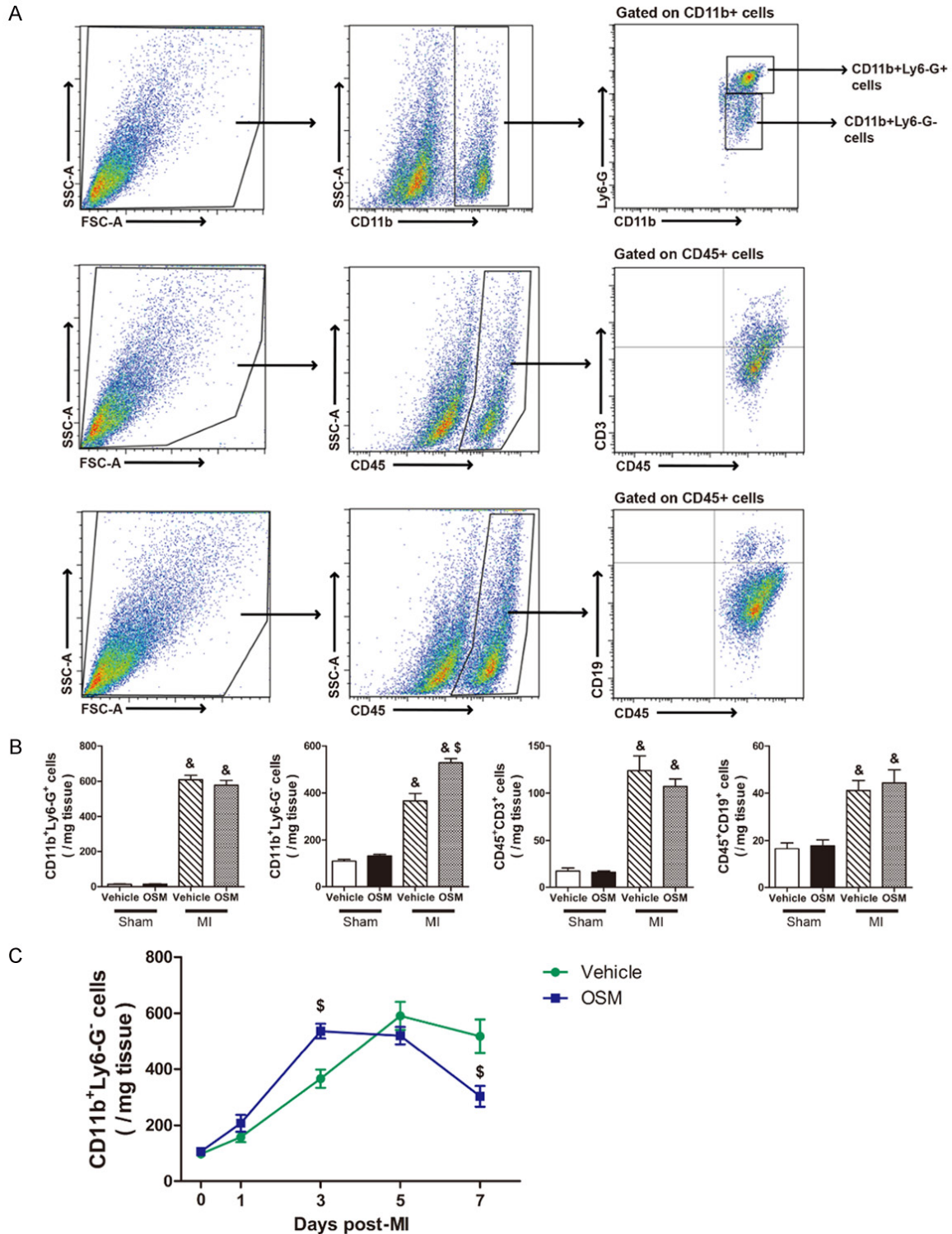


Figure 2. The oncostatin M (OSM) treatment influenced the accumulation of cardiac immune cells after myocardial infarction (MI). A. Gating strategies of the flow cytometry analysis of the cardiac neutrophils (CD11b⁺Ly6-G⁺ cells), macrophages/monocytes (CD11b⁺Ly6-G⁻ cells), T cells (CD45⁺CD3⁺ cells), and B cells (CD45⁺CD19⁺ cells). B. Quantitative analysis of the cardiac CD11b⁺Ly6-G⁺ cells, CD11b⁺Ly6-G⁻ cells, CD45⁺CD3⁺ cells, and the CD45⁺CD19⁺ cells in the sham + vehicle, sham + OSM, MI + vehicle, and MI + OSM mice 3 days after the surgeries. ^{&P}*P*<0.05 versus the sham + vehicle group (n=6). ^{&S}*P*<0.05 versus the MI + vehicle group (n=6). C. Time courses of the cardiac CD11b⁺Ly6-G⁺ cells in the MI + vehicle and the MI + OSM mice. ^{&P}*P*<0.05 versus the MI + vehicle group (n=6). The data are presented as the mean ± SEM.

Oncostatin M protects the myocardium against myocardial ischemia

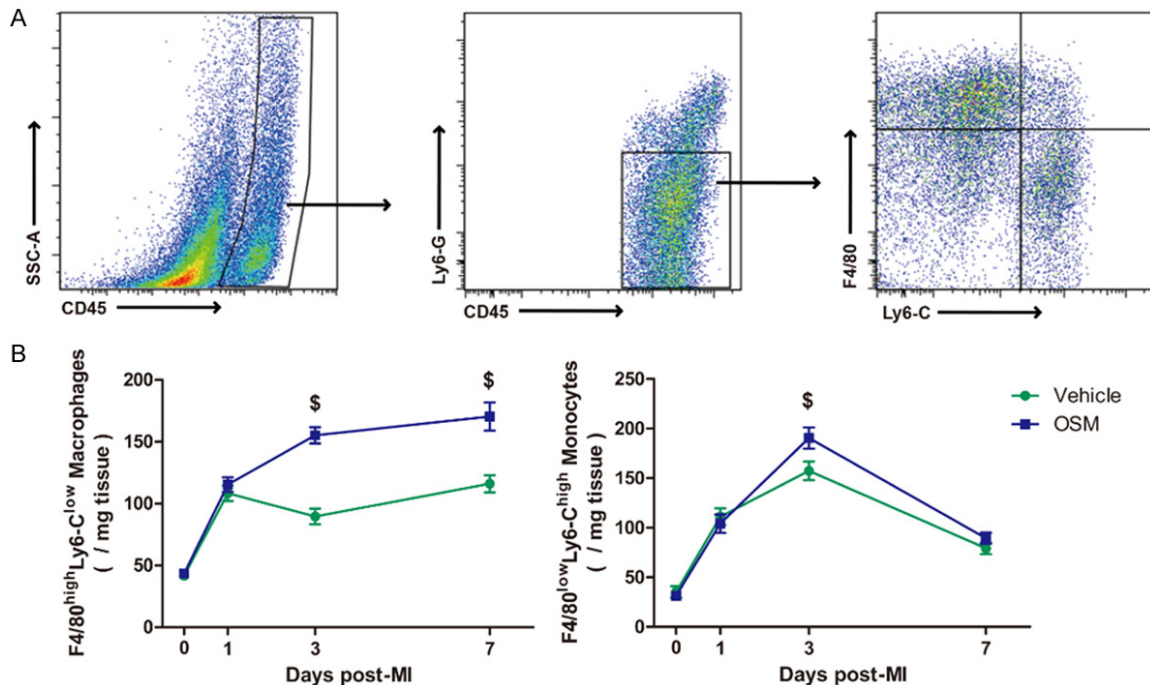


Figure 3. The oncostatin M (OSM) treatment influenced the accumulation of cardiac resident macrophages and recruited monocytes after myocardial infarction (MI). A. Gating strategies of the flow cytometry analysis of the cardiac resident macrophages ($CD45^+Ly6-G^-F4/80^{high}Ly6-C^{low}$ cells) and the recruited monocytes ($CD45^+Ly6-G^-F4/80^{low}Ly6-C^{high}$ cells). B. Time course of the cardiac $CD45^+Ly6-G^-F4/80^{high}Ly6-C^{low}$ cells and the $CD45^+Ly6-G^-F4/80^{low}Ly6-C^{high}$ cells in the MI + vehicle and the MI + OSM mice. $^{\$}P < 0.05$ versus the MI + vehicle group ($n = 6$). The data are presented as the mean \pm SEM.

for Windows (SPSS Inc., Chicago, IL, USA) was used for the data analysis.

Results

The OSM expressions in the post-MI hearts

The time courses of the OSM expressions in the post-MI hearts were measured using quantitative real-time PCR at the mRNA level. The OSM mRNA was significantly elevated by the MI surgery from day 3 and peaked at day 5 post-MI. Later, the OSM levels gradually waned toward the baseline (**Figure 1D**).

OSM treatment improves LV dysfunction and cardiac fibrosis following MI

Echocardiographic analyses were performed to examine the effect of OSM on the post-MI changes in cardiac structure and function (**Figure 1A**; [Supplementary Table 1](#)). For the sham mice, the echocardiography revealed no significant change in cardiac dilation, EF, or FS, irrespective of whether OSM treatment was given. Compared to the controls, the MI mice showed significant cardiac dilatation and a sig-

nificant reduction in LV function. The LVEDD and LVEDV in the MI + OSM mice were slightly lower than they were in the MI + vehicle mice, but with no significant differences. However, the deterioration of the LV function, indicated by EF and FS, was inhibited in the MI + OSM mice but not in the MI + vehicle mice.

Masson's trichrome stain was used to assess the fibrotic changes 2 weeks after the surgeries (**Figure 1B** and **1C**). The blue-stained (Masson's trichrome) areas were considered to indicate collagen deposition. No significant difference was observed in the positive Masson's trichrome-stained areas between the sham + vehicle and the sham + OSM mice. In the MI mice, the OSM treatment resulted in significantly decreased collagen content in both the border and infarct areas ([Supplementary Table 2](#)).

The OSM treatment influenced the dynamics of the cardiac monocytes/macrophages after MI

The innate immune response is an important regulator of post-MI cardiac repair. Flow cyto-

Oncostatin M protects the myocardium against myocardial ischemia

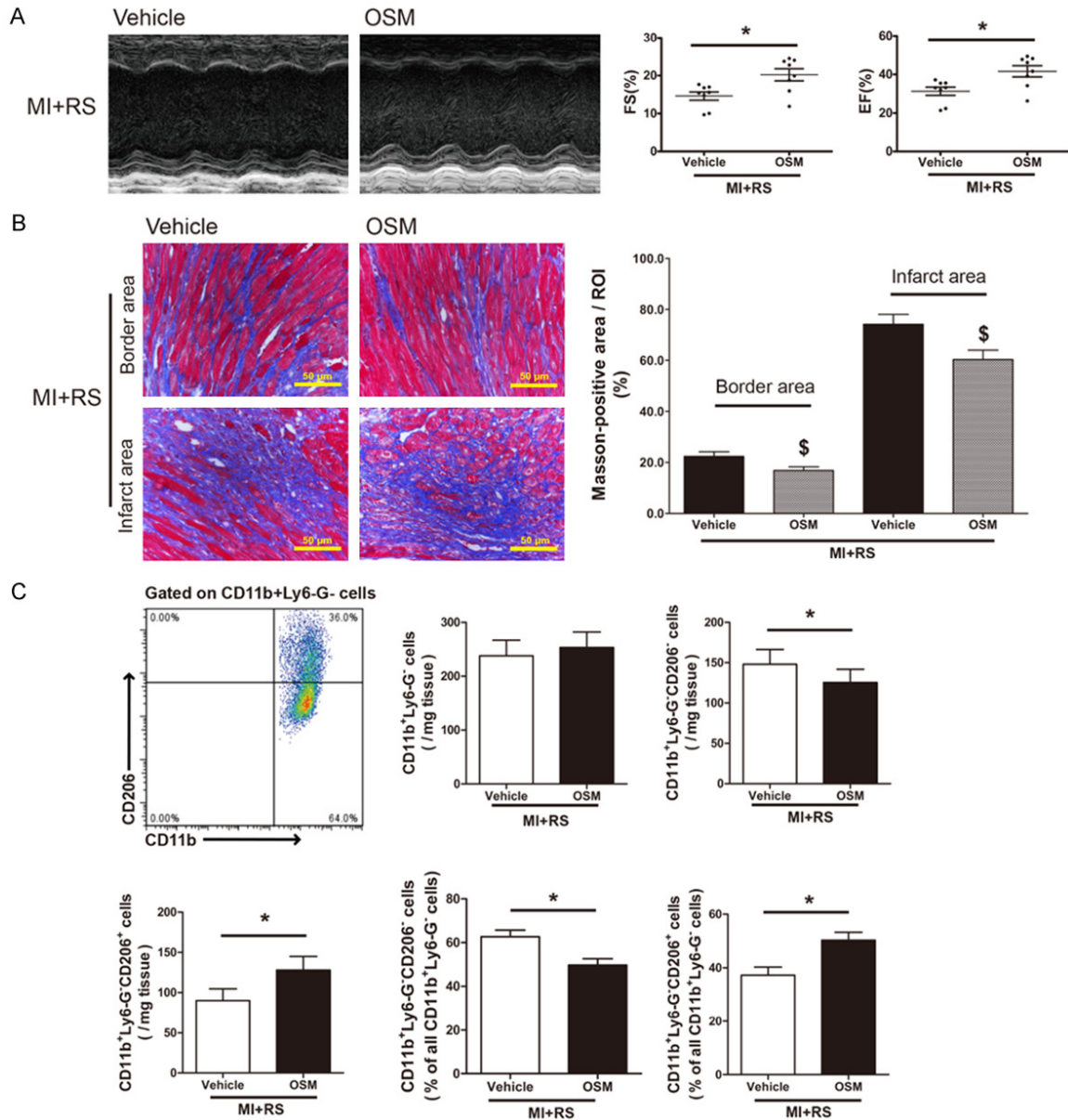


Figure 4. The oncostatin M (OSM) treatment contributed to the recovery of cardiac function and the M2 polarization of cardiac resident macrophages in the myocardial infarction (MI) mice treated with RS504393. **A.** Representative images of the M-mode echocardiograms and statistical analyses of FS and EF in the MI + vehicle and the MI + OSM mice treated with RS504393. * $P < 0.05$ ($n = 8$). **B.** Representative images and quantitative analysis of Masson's trichrome-stained sections in the hearts of the MI + vehicle and the MI + OSM mice treated with RS504393. * $P < 0.05$ ($n = 6$). The sections were photographed at 200 \times magnification. Scale bar = 50 μm . **C.** Gating strategies for the flow cytometry analysis and the quantitative analysis of the cardiac CD11b⁺Ly6-G⁻ cells, the CD11b⁺Ly6-G⁻CD206⁺ cells, and the CD11b⁺Ly6-G⁻CD206⁺ cells in the RS504393-treated MI + vehicle mice and the MI + OSM mice 3 days after the MI surgery. * $P < 0.05$ ($n = 6$). The data are presented as the means \pm SEM.

metric analyses were performed to evaluate the accumulation of the various inflammatory cells. Regardless of whether OSM was administered, the number of CD11b⁺Ly6-G⁻ neutrophils, CD11b⁺Ly6-G⁻ monocytes/macrophages, CD45⁺CD3⁺ T lymphocytes, and CD45⁺CD19⁺ B

lymphocytes were all significantly higher in the MI mice than in the sham mice on day 3 after the surgery. In the MI mice, the OSM treatment introduced more CD11b⁺Ly6-G⁻ cells into the infarct region (MI + vehicle, 366.13 \pm 32.36/mg tissue; MI + OSM, 536.50 \pm 26.33/mg tissue;

Oncostatin M protects the myocardium against myocardial ischemia

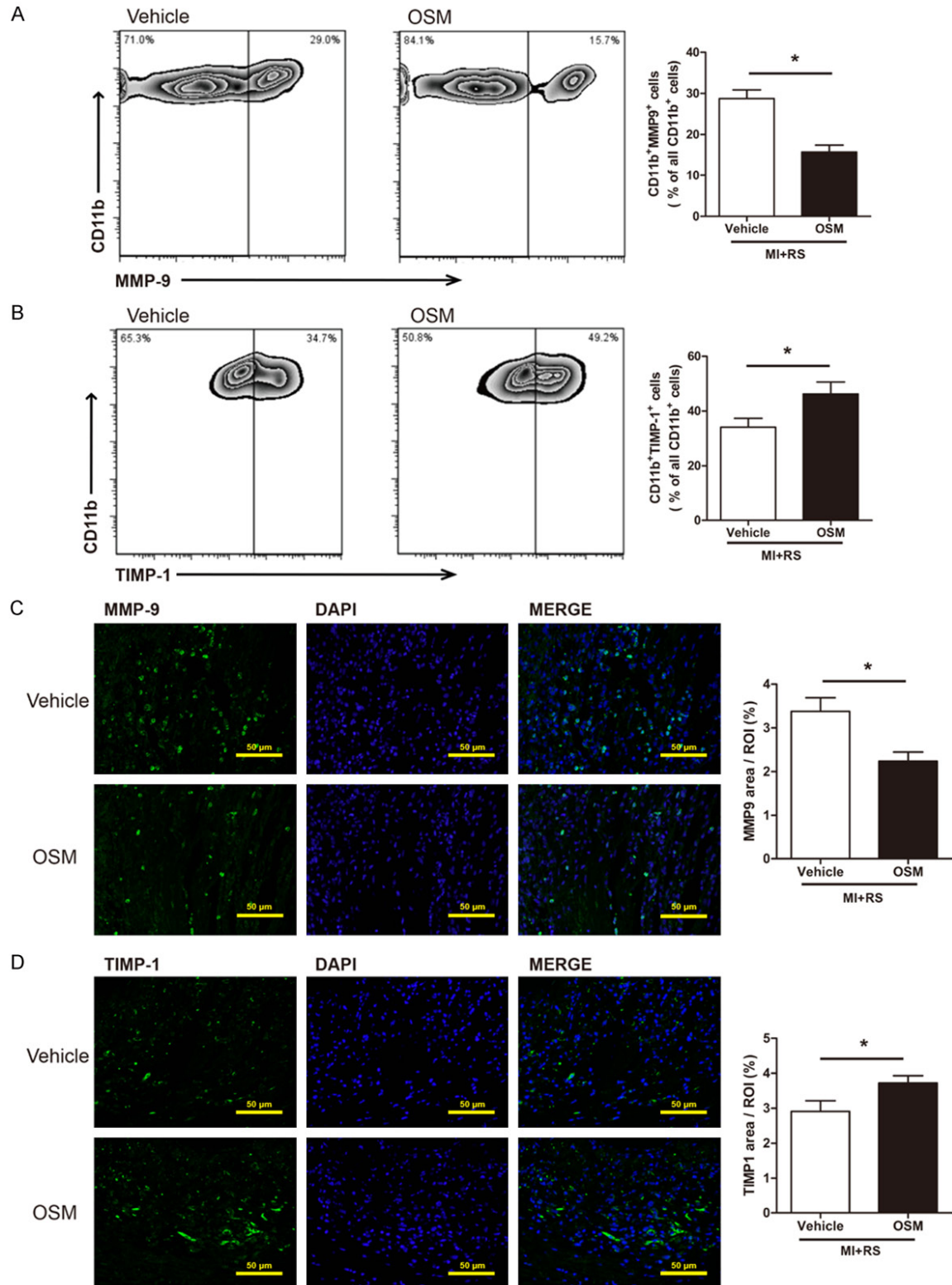


Figure 5. Oncostatin M (OSM) treatment improved the MMP/TIMP balance and the healing process in myocardial infarction (MI) mice treated with RS504393. **A.** Representative images of the flow cytometry analyses and a quantitative analysis of the cardiac CD11b⁺MMP-9⁺ cells in the MI + vehicle and the MI + OSM mice treated with RS504393. *P<0.05 (n=8). **B.** Representative images of the flow cytometry analyses and the quantitative analyses of the CD11b⁺TIMP-1⁺ cells in the MI + vehicle and the MI + OSM mice treated with RS504393. *P<0.05 (n=8). **C.** Representative images of the immunofluorescence and quantitative analyses for the MMP-9-stained sections in

Oncostatin M protects the myocardium against myocardial ischemia

the hearts of the MI + vehicle and the MI + OSM mice treated with RS504393. * $P < 0.05$ ($n = 6$). The sections were photographed at 200 \times magnification. Scale bar = 50 μm . D. Representative images of the immunofluorescence and quantitative analyses of the TIMP-1-stained heart sections of the MI + vehicle and MI + OSM mice treated with RS504393. * $P < 0.05$ ($n = 8$). The sections were photographed at 200 \times magnification. Scale bar = 50 μm .

$P < 0.05$; **Figure 2A** and **2B**). Next, the dynamics of the cardiac $\text{CD11b}^+\text{Ly6-G}^-$ cells were investigated in the MI + vehicle and MI + OSM mice. The peak values arrived earlier in the MI + OSM mice compared to the MI + vehicle mice (**Figure 2C**). A further analysis revealed that the time courses of both the $\text{CD45}^+\text{Ly6-G-F4/80}^{\text{high}}\text{Ly6-C}^{\text{low}}$ cells and the $\text{CD45}^+\text{Ly6-G-F4/80}^{\text{low}}\text{Ly6-C}^{\text{high}}$ cells were altered by the OSM administration following MI (**Figure 3**).

The OSM treatment improved the post-MI wound-healing process by regulating the polarization of the cardiac macrophages in the mice with blunted monocytic recruitment

RS504393 was used to suppress the CCR2 signaling pathway, thus inhibits the infiltration of the circulating monocytes into the infarct region. In the RS-treated mice, OSM still protected the heart from the deterioration of the LV performances, as indicated by the better EF and FS (**Figure 4A**; [Supplementary Table 3](#)). Similarly, the OSM treatment reduced the cardiac fibrosis both in the border and infarct areas (**Figure 4B**; [Supplementary Table 4](#)).

The macrophage polarization was further assessed using flow cytometry. In the RS-treated mice, OSM appeared to polarize the macrophages from an M1 to M2 phenotype. Specifically, the RS + MI + OSM mice had a higher frequency of $\text{CD11b}^+\text{Ly6-G-CD206}^+$ cells residing in the infarct area compared to the RS + MI + vehicle mice (**Figure 4C**).

The OSM treatment contributed to the rebalancing of the MMPs and TIMPs in the mice with blunted monocytic recruitment

Flow cytometry revealed that OSM reduced the numbers of the MMP-9^+ leucocytes and increased the numbers of the TIMP1^+ leucocytes, thus restoring the MMPs/TIMPs balance post-MI (**Figure 5A** and **5B**). These findings were further confirmed using an immunofluorescence analysis, with the RS + MI + OSM mice showing fewer MMP-9-stained areas and more TIMP-1-stained areas compared to the RS + MI + vehicle mice (**Figure 5C** and **5D**; [Supplementary Table 5](#)).

Discussion

It is well known that inflammation is essential during the repair process after AMI, but its timely resolution is necessary for favorable wound healing [16, 17]. In this study, OSM, a member of the IL-6 family of cytokines, was shown to regulate the cardiac macrophage accumulation and polarization of resident macrophages toward the reparative phenotype. As a result, OSM alleviated the loss of function and heart fibrosis after MI and therefore played a protective role in MI.

According to our results, the OSM expression was gradually up-regulated in the infarct region over the first 5 days after MI and then waned step by step. During this time, the cardiac macrophages/monocytes followed a similar dynamic curve. Additionally, the OSM administration shortened the time phase by which the number of monocytes/macrophages reaches the peak value. Thus, the OSM administration appeared to speed up the heart's wound healing process following MI, which is consistent with the results reported by Hu et al. [10].

We further explored the dynamics of the cardiac macrophages derived from the circulating monocytes or the locally self-renewed resident macrophages following AMI. We found that the number of resident macrophages ($\text{CD45}^+\text{Ly6-G-F4/80}^{\text{high}}\text{Ly6-C}^{\text{low}}$) was dramatically changed by the OSM treatment. To establish whether the recruited monocytes or the resident macrophages were the primary targets of OSM, we employed the CCR2 inhibitor RS504393 to impede the infiltration of the blood monocytes [18, 19]. Although the trafficking of the monocytes was hindered, the OSM benefits were reserved, as indicated by higher EF and FS, and reduced fibrosis both in the border and infarct regions in the post-MI hearts of the OSM-treated mice. These results imply that the resident macrophages are the key effectors of OSM in post-MI repair.

Macrophage polarization is a key process that balances the inflammatory response and the dissolution after cardiac injury. Following AMI,

Oncostatin M protects the myocardium against myocardial ischemia

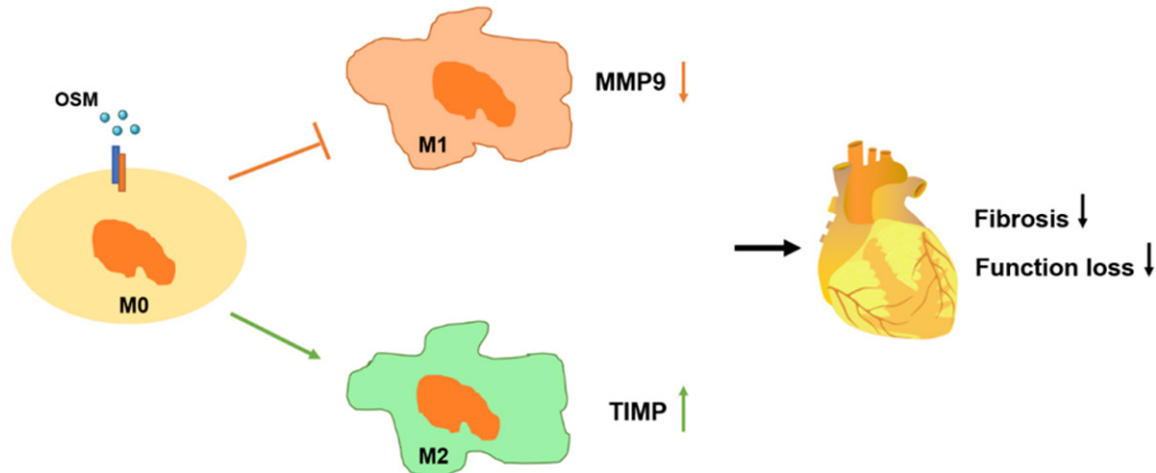


Figure 6. Schematic. OSM alleviates post-MI cardiac remodeling by polarizing the cardiac macrophages toward an M2 phenotype and correcting the MMP-9 and TIMP-1 balance.

macrophages initially show a pro-inflammatory M1 phenotype, which is later followed by an anti-inflammatory M2 phenotype; these phenotypes play distinct and even opposite roles in the immune response [20, 21]. M1 macrophages enhance the secretion of inflammatory cytokines, phagocytosis of cellular debris, and the reorganization of tissue matrices by producing MMPs [22]. In contrast, the M2 macrophages promote myofibroblast accumulation, angiogenesis, and collagen deposition [23, 24]. Thus, the prolonged presence of M1 macrophages can impede the resolution of inflammation and scar formation, while the M2 macrophages can facilitate neoangiogenesis and reconstruction. In our study, OSM administration promoted this post-MI polarization by increasing the CD206⁺ macrophage population residing in the infarct region. OSM administration also improved myocardial repair and function post-MI. This shift in balance from M1 to M2 macrophages might protect the heart from adverse remodeling following AMI [25, 26].

Further investigations confirmed the benefit of OSM in alleviating the maladaptive remodeling process. MMPs are a group of proteolytic enzymes that engage in the degradation of collagen and the extracellular matrix (ECM) components. The activity of the MMPs is tightly regulated by TIMPs, which can bind to the active site of the MMP enzymes and block access to their substrates [27]. During the reparative phase, a dynamic balance between MMPs and TIMPs is essential to ensure a suc-

cessful wound healing process by maintaining the integrity of the ECM. The induction of MMPs, the principal matrix-degrading proteinases, and the reduction in TIMPs is important in both early ischemic injury and late LV remodeling [28-30]. Previous studies have identified neutrophils as major producers of MMP-9 during the early phase of cardiac remodeling, but macrophages represent the main cellular source of TIMP-1 following MI [9]. In our study, OSM resulted in a reduction in MMP-9⁺ immune cells and an increase in TIMP-1⁺ immune cells in the infarct area in mice with blunted CCR2 signaling; these findings were reinforced by our immunofluorescence analyses. Therefore, OSM contributed to correcting the post-MI imbalance of the MMPs and TIMPs and protected against maladaptive remodeling.

In conclusion, we demonstrated that OSM contributes to the post-MI cardiac remodeling process and tends to shift the resident macrophage phenotype from the pro-inflammatory M1 macrophage to an anti-inflammatory M2 macrophage phenotype that resists adverse myocardial remodeling (**Figure 6**). In future studies, tissue-specific OSM gene knockout mice should be used to confirm the role of OSM, and the results should be further verified with human data. Despite these limitations, our study provides new insights into the roles of OSM in regulating cardiac macrophages in ischemic heart disease and thus represents a potential therapeutic strategy for the amelioration of the disease.

Acknowledgements

This work was supported by the National Natural Science Foundation of China (81800375, 81770249, and 81970330).

Disclosure of conflict of interest

None.

Address correspondence to: Dr. Ruiyan Zhang, Department of Cardiovascular Medicine, Ruijin Hospital, 197 Rui Jin 2nd Road, Shanghai 200025, P. R. China. Tel: +86-15216660998; E-mail: rjzhangruiyan@aliyun.com

References

- [1] Reed GW, Rossi JE and Cannon CP. Acute myocardial infarction. *Lancet* 2017; 389: 197-210.
- [2] Benjamin EJ, Blaha MJ, Chiuve SE, Cushman M, Das SR, Deo R, de Ferranti SD, Floyd J, Fornage M, Gillespie C, Isasi CR, Jimenez MC, Jordan LC, Judd SE, Lackland D, Lichtman JH, Lisabeth L, Liu S, Longenecker CT, Mackey RH, Matsushita K, Mozaffarian D, Mussolino ME, Nasir K, Neumar RW, Palaniappan L, Pandey DK, Thiagarajan RR, Reeves MJ, Ritchey M, Rodriguez CJ, Roth GA, Rosamond WD, Sasson C, Towfighi A, Tsao CW, Turner MB, Virani SS, Voeks JH, Willey JZ, Wilkins JT, Wu JH, Alger HM, Wong SS and Muntner P; American Heart Association Statistics Committee and Stroke Statistics Subcommittee. Heart disease and stroke statistics-2017 update: a report from the American Heart Association. *Circulation* 2017; 135: e146-e603.
- [3] Bianco V, Kilic A, Gleason TG, Aranda-Michel E, Wang Y, Navid F and Sultan I. Timing of coronary artery bypass grafting after acute myocardial infarction may not influence mortality and readmissions. *J Thorac Cardiovasc Surg* 2021; 161: 2056-2064, e4.
- [4] Dondo TB, Hall M, West RM, Jernberg T, Lindahl B, Bueno H, Danchin N, Deanfield JE, Hemingway H, Fox KAA, Timmis AD and Gale CP. beta-blockers and mortality after acute myocardial infarction in patients without heart failure or ventricular dysfunction. *J Am Coll Cardiol* 2017; 69: 2710-2720.
- [5] Chen J, Hsieh AF, Dharmarajan K, Masoudi FA and Krumholz HM. National trends in heart failure hospitalization after acute myocardial infarction for Medicare beneficiaries: 1998-2010. *Circulation* 2013; 128: 2577-2584.
- [6] Hermanns HM. Oncostatin M and interleukin-31: cytokines, receptors, signal transduction and physiology. *Cytokine Growth Factor Rev* 2015; 26: 545-558.
- [7] Adrian-Segarra JM, Schindler N, Gajawada P, Lorchner H, Braun T and Poling J. The AB loop and D-helix in binding site III of human Oncostatin M (OSM) are required for OSM receptor activation. *J Biol Chem* 2018; 293: 7017-7029.
- [8] Kubin T, Poling J, Kostin S, Gajawada P, Hein S, Rees W, Wietelmann A, Tanaka M, Lorchner H, Schimanski S, Szibor M, Warnecke H and Braun T. Oncostatin M is a major mediator of cardiomyocyte dedifferentiation and remodeling. *Cell Stem Cell* 2011; 9: 420-432.
- [9] Lorchner H, Poling J, Gajawada P, Hou Y, Polyakova V, Kostin S, Adrian-Segarra JM, Boettger T, Wietelmann A, Warnecke H, Richter M, Kubin T and Braun T. Myocardial healing requires Reg3beta-dependent accumulation of macrophages in the ischemic heart. *Nat Med* 2015; 21: 353-362.
- [10] Hu J, Zhang L, Zhao Z, Zhang M, Lin J, Wang J, Yu W, Man W, Li C, Zhang R, Gao E, Wang H and Sun D. OSM mitigates post-infarction cardiac remodeling and dysfunction by up-regulating autophagy through Mst1 suppression. *Biochim Biophys Acta Mol Basis Dis* 2017; 1863: 1951-1961.
- [11] Abe H, Takeda N, Isagawa T, Semba H, Nishimura S, Morioka MS, Nakagama Y, Sato T, Soma K, Koyama K, Wake M, Katoh M, Asagiri M, Neugent ML, Kim JW, Stockmann C, Yonezawa T, Inuzuka R, Hirota Y, Maemura K, Yamashita T, Otsu K, Manabe I, Nagai R and Komuro I. Macrophage hypoxia signaling regulates cardiac fibrosis via Oncostatin M. *Nat Commun* 2019; 10: 2824.
- [12] Ma Y, Yabluchanskiy A, Iyer RP, Cannon PL, Flynn ER, Jung M, Henry J, Cates CA, DeLeon-Pennell KY and Lindsey ML. Temporal neutrophil polarization following myocardial infarction. *Cardiovasc Res* 2016; 110: 51-61.
- [13] Yan X, Zhang H, Fan Q, Hu J, Tao R, Chen Q, Iwakura Y, Shen W, Lu L, Zhang Q and Zhang R. Dectin-2 deficiency modulates Th1 differentiation and improves wound healing after myocardial infarction. *Circ Res* 2017; 120: 1116-1129.
- [14] Han H, Zhu J, Zhu Z, Ni J, Du R, Dai Y, Chen Y, Wu Z, Lu L and Zhang R. p-Cresyl sulfate aggravates cardiac dysfunction associated with chronic kidney disease by enhancing apoptosis of cardiomyocytes. *J Am Heart Assoc* 2015; 4: e001852.
- [15] Fan Q, Tao R, Zhang H, Xie H, Lu L, Wang T, Su M, Hu J, Zhang Q, Chen Q, Iwakura Y, Shen W, Zhang R and Yan X. Dectin-1 Contributes to myocardial ischemia/reperfusion injury by regulating macrophage polarization and neutrophil infiltration. *Circulation* 2019; 139: 663-678.

Oncostatin M protects the myocardium against myocardial ischemia

- [16] Ma Y, Mouton AJ and Lindsey ML. Cardiac macrophage biology in the steady-state heart, the aging heart, and following myocardial infarction. *Transl Res* 2018; 191: 15-28.
- [17] Bonaventura A, Montecucco F and Dallegri F. Cellular recruitment in myocardial ischaemia/reperfusion injury. *Eur J Clin Invest* 2016; 46: 590-601.
- [18] Dewald O, Zymek P, Winkelmann K, Koerting A, Ren G, Abou-Khamis T, Michael LH, Rollins BJ, Entman ML and Frangogiannis NG. CCL2/monocyte chemoattractant protein-1 regulates inflammatory responses critical to healing myocardial infarcts. *Circ Res* 2005; 96: 881-889.
- [19] Jung K, Kim P, Leuschner F, Gorbato R, Kim JK, Ueno T, Nahrendorf M and Yun SH. Endoscopic time-lapse imaging of immune cells in infarcted mouse hearts. *Circ Res* 2013; 112: 891-899.
- [20] Gombozhapova A, Rogovskaya Y, Shurupov V, Rebenkova M, Kzhyshkowska J, Popov SV, Karpov RS and Ryabov V. Macrophage activation and polarization in post-infarction cardiac remodeling. *J Biomed Sci* 2017; 24: 13.
- [21] Yan X, Anzai A, Katsumata Y, Matsuhashi T, Ito K, Endo J, Yamamoto T, Takeshima A, Shinmura K, Shen W, Fukuda K and Sano M. Temporal dynamics of cardiac immune cell accumulation following acute myocardial infarction. *J Mol Cell Cardiol* 2013; 62: 24-35.
- [22] Troidl C, Mollmann H, Nef H, Masseli F, Voss S, Szardien S, Willmer M, Rolf A, Rixe J, Troidl K, Kostin S, Hamm C and Elsasser A. Classically and alternatively activated macrophages contribute to tissue remodelling after myocardial infarction. *J Cell Mol Med* 2009; 13: 3485-3496.
- [23] Dutta P and Nahrendorf M. Monocytes in myocardial infarction. *Arterioscler Thromb Vasc Biol* 2015; 35: 1066-1070.
- [24] Ishikawa S, Noma T, Fu HY, Matsuzaki T, Ishizawa M, Ishikawa K, Murakami K, Nishimoto N, Nishiyama A and Minamino T. Apoptosis inhibitor of macrophage depletion decreased M1 macrophage accumulation and the incidence of cardiac rupture after myocardial infarction in mice. *PLoS One* 2017; 12: e0187894.
- [25] Weirather J, Hofmann UD, Beyersdorf N, Ramos GC, Vogel B, Frey A, Ertl G, Kerkau T and Frantz S. Foxp3+ CD4+ T cells improve healing after myocardial infarction by modulating monocyte/macrophage differentiation. *Circ Res* 2014; 115: 55-67.
- [26] Courties G, Heidt T, Sebas M, Iwamoto Y, Jeon D, Truelove J, Tricot B, Wojtkiewicz G, Dutta P, Sager HB, Borodovsky A, Novobrantseva T, Klebanov B, Fitzgerald K, Anderson DG, Libby P, Swirski FK, Weissleder R and Nahrendorf M. In vivo silencing of the transcription factor IRF5 reprograms the macrophage phenotype and improves infarct healing. *J Am Coll Cardiol* 2014; 63: 1556-1566.
- [27] Kaludercic N, Lindsey ML, Tavazzi B, Lazzarino G and Paolocci N. Inhibiting metalloproteases with PD 166793 in heart failure: impact on cardiac remodeling and beyond. *Cardiovasc Ther* 2008; 26: 24-37.
- [28] Thorn SL, Barlow SC, Feher A, Stacy MR, Doviak H, Jacobs J, Zellars K, Renaud JM, Klein R, deKemp RA, Khakoo AY, Lee T, Spinale FG and Sinusas AJ. Application of hybrid matrix metalloproteinase-targeted and dynamic (201) Tl single-photon emission computed tomography/computed tomography imaging for evaluation of early post-myocardial infarction remodeling. *Circ Cardiovasc Imaging* 2019; 12: e009055.
- [29] Iyer RP, Jung M and Lindsey ML. MMP-9 signaling in the left ventricle following myocardial infarction. *Am J Physiol Heart Circ Physiol* 2016; 311: H190-198.
- [30] Cheng Z, Ou L, Liu Y, Liu X, Li F, Sun B, Che Y, Kong D, Yu Y and Steinhoff G. Granulocyte colony-stimulating factor exacerbates cardiac fibrosis after myocardial infarction in a rat model of permanent occlusion. *Cardiovasc Res* 2008; 80: 425-434.

Oncostatin M protects the myocardium against myocardial ischemia

Supplementary Table 1. Data of M-mode echocardiograms and statistical analysis

	Sham + vehicle	MI + vehicle	Sham + OSM	MI + OSM
LVEDD (mm)	3.05±0.17	4.24±0.45 ^a	2.90±0.18	4.04±0.41
LVEDV (μL)	36.56±4.86	81.97±21.99 ^a	32.36±4.98	72.65±17.33
LVEDS (mm)	1.635±0.13	3.674±0.35	1.578±0.163	3.273±0.32
LVESV (μL)	7.671±1.64	57.87±13.69	7.036±1.91	43.87±10.45
EF (%)	79.18±2.17	28.56±5.67 ^a	78.35±4.43	39.57±2.16 ^b
FS (%)	46.43±2.05	13.25±2.94 ^a	45.61±4.08	18.95±1.20 ^b

LVEDD, left-ventricle end-diastolic diameter; LVEDV, left-ventricle end-diastolic volume; LVEDS, left-ventricle end-systolic diameter; LVESV, left-ventricle end-systolic volume; EF, ejection fraction; FS, fractional shortening. ^ap<0.05 compared to sham + vehicle, ^bp<0.05 compared to MI + vehicle.

Supplementary Table 2. Data of Masson's trichrome-stained sections

	Sham + vehicle	Sham + OSM	MI + vehicle (border area)	MI + OSM (border area)	MI + vehicle (infarct area)	MI + OSM (infarct area)
Masson's trichrome stained areas (%)	0.62±0.08%	0.87±0.10%	29.17±2.56%	21.00±1.16% ^a	79.33±4.66%	64.17±2.39% ^b

^ap<0.05 compared to MI + vehicle (border area), ^bp<0.05 compared to MI + vehicle (infarct area).

Supplementary Table 3. Data of M-mode echocardiograms and statistical analysis for Experiment 2

	RS + MI + vehicle	RS + MI + OSM	<i>p</i>
EF	31.31±6.02%	41.60±8.09%	<0.05
FS	14.61±3.08%	20.21±4.51%	<0.05

Supplementary Table 4. Data of Masson's trichrome-stained sections for Experiment 2

	RS + MI + vehicle (border area)	RS + MI + OSM (border area)	RS + MI + vehicle (infarct area)	RS + MI + OSM (infarct area)
Masson's trichrome stained areas (%)	22.33±1.59%	16.83±1.21% ^a	74.17±3.36%	60.33±3.20% ^b

^ap<0.05 compared to RS + MI + vehicle border area, ^bp<0.05 compared to RS + MI + OSM infarct area.

Supplementary Table 5. Data for quantitative analysis for MMP-9/TIMP-stained area in infarcted hearts

	RS + MI + vehicle (infarct area)	RS + MI + OSM (infarct area)	<i>p</i>
MMP-9 area/ROI%	3.38±0.31%	2.24±0.21%	<0.05
TIMP-1 area/ROI%	2.91±0.31%	3.73±0.21%	<0.05